The Discovery of a Selective, Small Molecule Agonist for the Mas-Related Gene X1 Receptor

Berthold Wroblowski, Mark J. Wigglesworth, Philip G. Szekeres, Graham D. Smith, Shahzad S. Rahman, Neville H. Nicholson,* Alison I. Muir, Adrian Hall, Jag P. Heer, Stephen L. Garland, and William J. Coates

GlaxoSmithKline Pharmaceuticals, New Frontiers Science Park (North), Third Avenue, Harlow, Essex CM19 5AW, United Kingdom

The novel 7-transmembrane receptor MrgX1 is located predominantly in the dorsal root ganglion and has consequently been implicated in the perception of pain. Here we describe the discovery and optimization of a small molecule agonist and initial docking studies of this ligand into the receptor in order to provide a suitable lead and tool compound for the elucidation of the physiological function of the receptor.

Introduction

Pain, especially in the terminally ill, remains a tragic and unresolved medical dilemma. Despite the plethora of approaches to a solution[1,2] encompassing ion channels,[3-7] 7-transmembrane receptors,[8,9] and holism,[10,11] opiates such as morphine remain the treatment of choice for the relief of acute pain.[12,13] However, the analgesic effect of morphine declines and adverse effects increase with prolonged exposure, and this limits its use to transitory, postoperative pain or, in escalating doses, to the final days of disease.

The recently described Mas-related genes (Mrg) or sensory neuron-specific receptors, are a family of 7-transmembrane receptors that have been implicated in the perception of pain through their expression in small afferent nerve fibers of the dorsal root ganglion.[14,15] Data from the rat have suggested that painful stimuli are intensified by the presence of an Mrg agonist in the cerebrospinal fluid and that an Mrg antagonist might therefore give protection against painful stimuli.[16] A member of this family of receptors, MrgX1[a] has been identified in the human, but the high frequency of significant changes within these genes shows that they are undergoing rapid evolution[17,18] and, as a consequence, the closest rat gene has only 60% identity. Functional and structural homologues more closely related to the human gene have been identified in the rhesus[19] and macaque[20] monkeys and screening for MrgX1 antagonists was initiated[21,22] to enable studies of the function of these receptors, but there have been no more specific reports linking MrgX1 antagonists to the amelioration of pain in higher mammals.

However, recent publications[23] have shown that an Mrg agonist is able to reactivate the analgesic effect of morphine after it has ceased to be effective due to prolonged use (tolerance). Intrathecal administration of bovine adrenal medulla 8–22 (BAM8–22), a selective small peptide agonist at Mrg receptors, did not by itself directly affect acute thermal nociception in the rat. However, when chronic morphine administration was intermittently supplemented with BAM8–22, the antinociception due to the morphine was prolonged. Furthermore, intermittent administration of BAM8–22 consistently reversed established morphine tolerance.

The reversal of morphine tolerance was described over 30 years ago,[24] and several mechanisms, including NMDA receptors[25,26] and PKA,[27] GSK3,[28] and PKC[29] kinases, have been invoked to explain the phenomenon that has also been reported to emanate from the spinal column.[30] Chen et al.[31] have recently suggested that activation of rat MrgX receptors induces spinal analgesia by suppressing NMDA receptor-mediated activation of spinal dorsal horn neurons and increasing NOS activity.

Stimulation of MrgX1 is an alternative mechanism for the reversal of morphine tolerance and provides a target that is a simple 7-transmembrane receptor that has no known function other than its putative role in pain and is limited in its occurrence to the dorsal root ganglion. This mechanism requires an MrgX1 agonist, whereas the reversal of morphine tolerance by direct antagonism of the NMDA receptor requires a ligand with a high affinity for a widely distributed receptor.

These data have generated a consequent interest in novel, pharmaceutically acceptable MrgX1 agonists,[32] and we describe here the discovery, synthesis, and optimization of a small molecule agonist and initial docking studies of the ligand into the receptor.

High Throughput Screening

The GlaxoSmithKline compound collection was screened using HEK293 cells stably transfected with human MrgX1 in an intracellular calcium mobilization assay with the fluorometric imaging plate reader (FLIPR, Molecular Devices) essentially as described by Sulivan et al.[33] This gave 79 compounds comprising several different chemotypes that had an intrinsic activity greater than 0.25 of that of the standard BAM6–22. Among the most active of these was a series of pyridazinones represented by **1**, which appeared to be readily synthesized and amenable to variation using precursors immobilized on resin or in solution phase.

The high throughput screening hit was resynthesized using the route shown in Scheme 1. The 5-chlorine of commercially available 4,5-dichloropyridazin-3-one **2** was displaced regioselectively with piperazine to give fragment **3**. ¹H NMR and NOE experiments were consistent with the proposed regiochemistry of compound **3** but not definitive, so the remaining chlorine was hydrogenated to give compound **3a**, which was shown to have the required regiochemistry. The amine **3** was attached to Wang resin through a carbamate linkage to give the immobilized reagent **4**, which was reacted with 2-methyl-3-nitrobenzylbromide in the presence of a strong base. An aliquot of the product **5** was liberated from the resin with TFA to provide the soluble

---

* To whom correspondence should be addressed. Phone and Fax: 0(44) 1440 730580. E-mail: nxnicholson@gmail.com.

a Abbreviations: MrgX1, mas-related gene X1; BAM, bovine adrenal medulla; DRR, dorsal root receptor; NMDA, *N*-methyl-D-aspartate; 5-HT, 5-hydroxytryptamine; HOAt, 3*H*-[1,2,3]triazolo[4,5-*b*]pyridin-3-ol; IA, intrinsic activity; DMSO, dimethylsulfoxide; TFA, trifluoroacetic acid; DMF, dimethylformamide; THF, tetrahydrofuran; NMP, *N*-methylpyrollidinone.

Scheme 1[a]
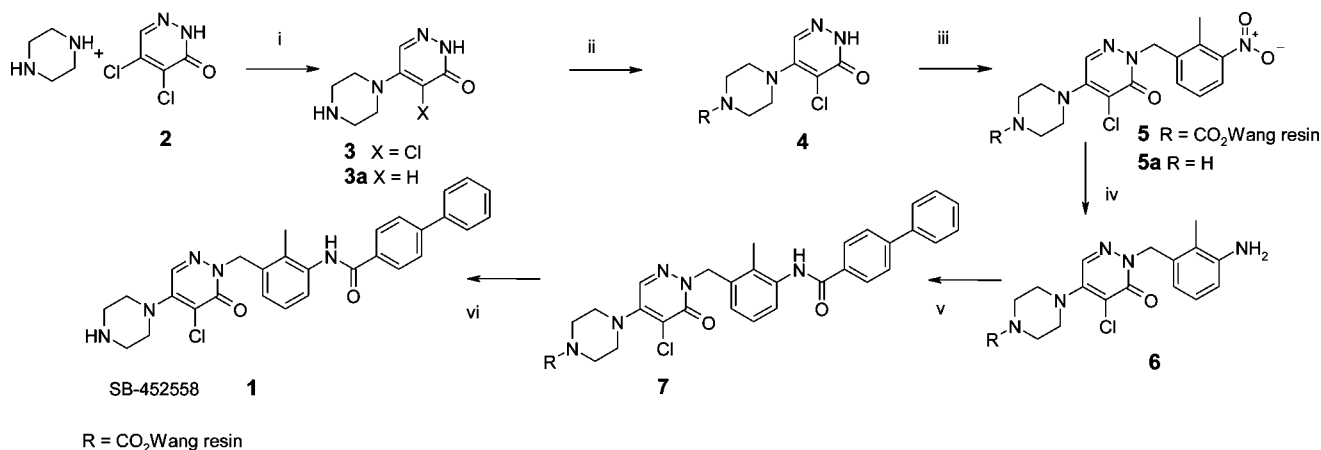
[a] Reagents and conditions: (i) EtOH, 90 °C; (ii) 2-pyridylcarboxy−Wang resin; (iii) 2-methyl-3-nitrobenzylbromide, tetramethylguanine; (iv) SnCl$_2$.2H$_2$O, NMP; (v) 4-biphenylcarboxylic acid, HOAt, DIC, DMF/MDC 1/1; (vi) 20% TFA /DCM.

Table 1. The Affinity of the Pyridazinones for Aminergic Receptors[a]

						pK$_i$							pEC$_{50}$
			5-HT						α	β	dopamine		Mrg
R1	R2	compd	1B	1D	2A	2B	2C	6	1B	2	D2	D3	X1
H	H	**8**	6.28	6.38	7.22	6.81	7.52	6.31	6.2	5.64	5.28	6.09	5.08
H	CH$_3$	**9**	6.11	6.13	8.67	7.52	8.41	6.08	6.25	5.62	5.31	6.11	5.39
CH$_3$	H	**1**	6.23	6.34	7.28	7.01	6.52	5.47	5.84	<5.2	5.29	5.45	6.9

[a] The standard deviation was less than 0.35 for between 2 and 6 replicates. The cell line for 5-HT2 receptors was HEK293 for 5-HT6, HELA, and for all other receptors CHO. Ligands were: 5-HT1B and D and 5-HT2B, ^{3}H 5-HT; 5-HT6, ^{3}H LSD; 5-HT2A, ^{3}H ketanserin; 5-HT2C, ^{3}H mesulergine; α1B, ^{3}H Prazosin; β2, ^{125}I iodocyanopindolol; D2 and D3, ^{125}I iodosulpride. pK$_i$ = −log 10 K$_i$, where K$_i$ is calculated using the Cheng−Prusoff equation IC$_{50}$/1 + ([free radioligand]/[the dissociation constant]).

compound **5a**, which was analyzed by ^{1}H and ^{13}C NMR to ensure that alkylation had occurred at the required position. The carbon shift of the benzyl CH$_2$ at 53 ppm was consistent with *N*-alkylation rather than *O*-alkylation and HMBC correlations confirmed N2 as the site of alkylation. The nitro moiety of resin bound **5** was reduced with tin chloride, and the resulting amine **6** was coupled with 4-phenylbenzoic acid to provide compound **7**, which, on cleavage from the resin with TFA, gave the target compound **1**.

Testing of the pure **1** confirmed its MrgX1 agonist activity (pEC$_{50}$ = 6.9, intrinsic activity 0.7 relative to BAM3200), and initial SAR of the core of the molecule was available from compounds already in the GlaxoSmithKline collection. Excision of the methyl from the central benzene ring to give compound **8** or moving it to the *ortho*-position on the alternate side of the amide, compound **9**, reduced potency 15-fold (Table 1). Placing the amide in the ortho- or para- positions of the central benzene ring caused a similar decrease in potency. Clearly, the preferred agonist conformation required the amide side chain to be extended with the amide carbonyl away from the methyl group of **1**. Consequently, this methyl, together with the rest of the benzylpyridazinone core, were adopted to investigate the SAR of the periphery of the molecule.

Aminergic activity was clearly adumbrated by the positive charge at physiological pH in the selected structures, and this was confirmed for three members of the series that displayed high affinities for 5-HT2 A, B, and C receptors and moderate

affinity for 5-HT1 B and D, α1B and β2 adrenoreceptors and for dopamine D2 and D3 receptors (Table 1).

Receptor Modeling Studies

A model of the MrgX1 receptor was built in order to facilitate chemical optimization of the ligand. The protein structure was modeled by homology to the published bovine rhodopsin crystal structure (PDB code 1f88) using the Modeler software.[34] The hit structure **1** and a series of closely related compounds were docked in using FLO.[35] This allowed conformational flexibility in both the ligand and amino acid side-chains of the binding pocket. The partial charges of the ligand had been precalculated using Vamp[36] to obtain a more realistic charge distribution than the default.

In the modes with the highest docking scores, the compounds exhibited well-defined interactions of the charged piperazine nitrogen with the acidic residues E157 of TM4 and/or D177 of TM5. The pyridazinone portion of the structure sat high up in the receptor in an approximately horizontal orientation, contacting residues from the second extracellular loop. The ligand then turned about the benzyl amide section, with the biphenyl part running vertically downward into a hydrophobic pocket between TMs 3 and 6 (Figure 1).

The rhodopsin structure is of the inactive state of the receptor. We considered whether to invoke some specific changes in the model to account for the fact that the ligands are agonists rather than antagonists. Typically, this might involve movement of a key W residue that changes conformation as part of the "toggle
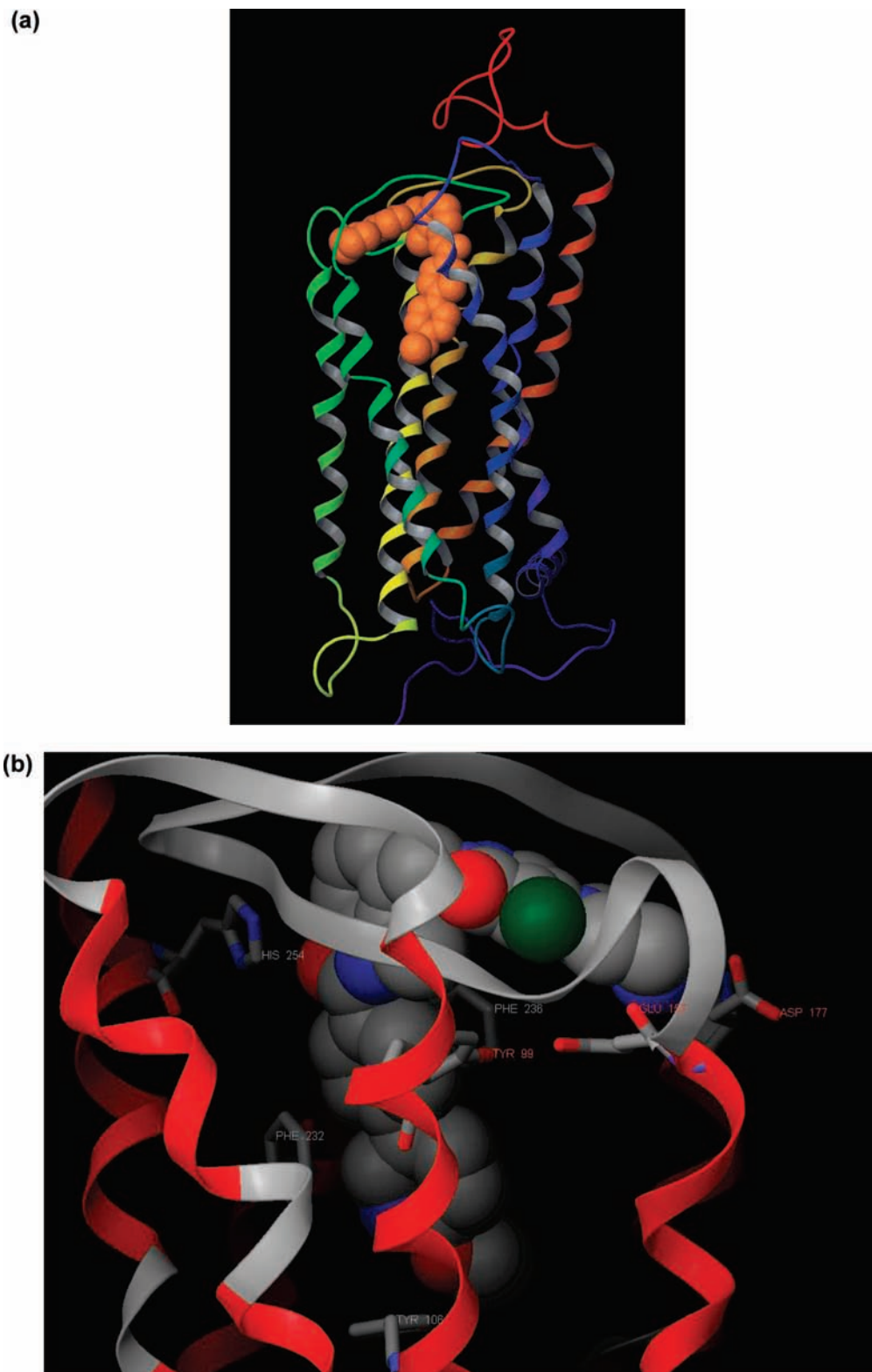
Figure 1. (a) Position of compound **22** (shown in orange space fill) as modeled in the MrgX1 receptor bundle. The transmembrane helices run from TM1 shown in red through to TM7 shown in dark blue. The ligand is anchored on TMs 4 and 5 (yellow/green and green/blue) via two charge−charge interactions and then forms a series of π-stacking interactions with aromatic residues of TMs 3 (yellow), 6 and 7 (light blue and dark blue). (b) Close up view of compound **22** (shown in space fill) as modeled in the MrgX1 receptor bundle. Key interactions are formed with Tyr 99, Tyr 106, Glu 157, Asp 177, Phe 232, Phe 236, and His 254.

switch" model[37] of receptor activation. However, this cannot be applied here. The "switch", usually afforded by the W on TM6 as part of a CWLP sequence, is replaced by a G in MrgX1. Rather than tripping the switch to alleviate the steric constraint and hence allow TMs 3 and 6 to come closer together, it may be that the ligands form a series of favorable interactions with residues along each side that serves to draw TM3 and TM6 closer together on the extracellular side. It is noticeable that the biaryl portion contacts a number of aromatic residues from TMs 3 (Y99, Y106) and 6 (F232, F236), and it is possible that

Scheme 2[a]
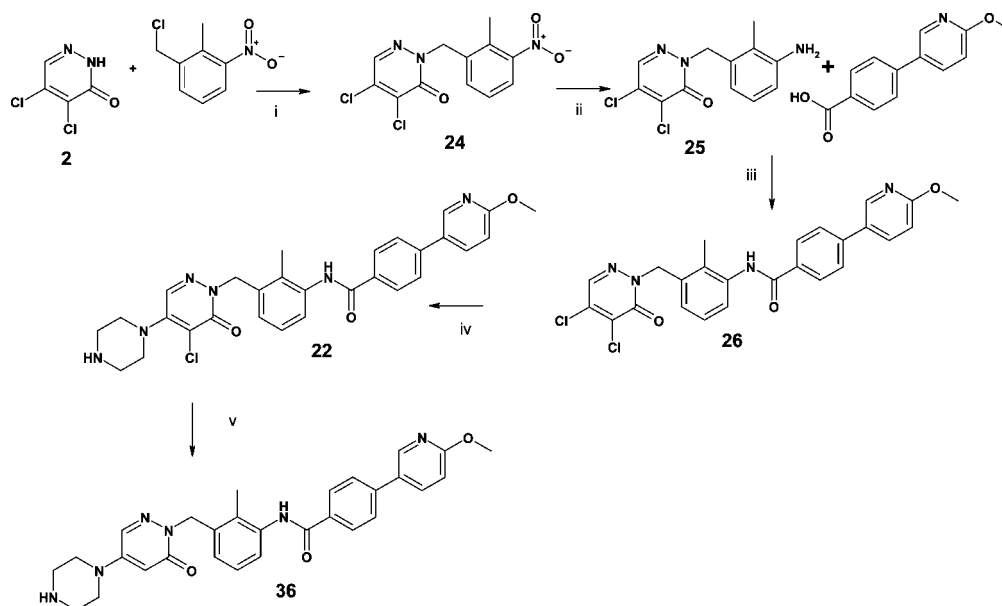
[a] Reagents and conditions: (i) tetramethylguanine, THF; (ii) SnCl$_2$·2H$_2$O, EtOH; (iii) 4-[6-(methyloxy)-3-pyridinyl]benzoic acid, HOAt, DIC, DMF/MDC 1/1; (iv) piperazine; (v) hydrazine, 10% Pd−C.

the interactions with these residues are improved in an activated form of the receptor. The H254 residue from TM7 is also in reasonable proximity to the ligands but may improve its interaction if the top of the helix were to come closer to TM3. As it was, we found that the ligands fitted well in the receptor bundle as modeled based on the available crystal structure without any explicit change to account for modality.

The modeling was used to identify structural changes that would increase MrgX1 affinity and also to consider issues around selectivity. The acidic side chains at the tops of TMs 4 and 5 in MrgX1 are not preserved in the aminergic receptors. The equivalent positions in 5-HT2C, for example, are both I residues. Hence, the ligands probably do not bind in the same mode at aminergic receptors and are perhaps more likely to anchor on the key D residue of TM3 usually implicated in small molecule binding. Thus, rather than focus on specific differences between MrgX1 and the aminergic receptors for selectivity, we sought opportunities to improve the potency at the target receptor in the expectation that this would also serve to drive divergent SAR. In particular, these studies suggested the incorporation of heteroatoms into the distal ring of the biphenyl moiety might enhance binding to the MrgX1 receptor by forming hydrogen bonding interactions, particularly in the region of the hydroxyl group of Y106. A series of compounds was synthesized using biaryl acids to investigate this possibility.

Optimization of the Biaryl Moiety. The route shown in Scheme 1 was employed; 4-biphenyl carboxylic acid being replaced in the penultimate step by a series of acids to produce the compounds shown in Table 2.

The results indicate that small alkyl (compound **10**) or small aryl (compounds **11** and **12**) amides provide an inadequate hydrophobic surface to bind to MrgX1 and that the high concentration at which the ligands bind gives poor intrinsic activity. Increasing the bulk of the hydrophobe (compound **13**) improves the potency but not the intrinsic activity, and this can be rationalized in our model by an improvement in the binding of the ligand. However, extending the hydrophobic moiety has a positive effect on the potency and the removal of bulky substituents close to the amide increases intrinsic activity (compound **14**).

Table 2. The Effect of Variation of the Amide Substituent on MrgX1 Activity[a]
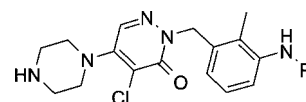
Compd	R	pEC$_{50}$	IA	Compd	R	pEC$_{50}$	IA
10		4.58	0.47	**11**		4.68	0.55
12		4.70	0.37	**13**		4.96	0.28
14		5.57	0.5	**15**		6.23	0.63
16		6.84	0.69	**17**		5.09	0.58
18		5.38	0.60	**19**		6.88	0.71
20		6.54	0.82	**21**		6.40	0.80
22		7.62	0.67	**23**		7.28	0.69
	BAM3200	6.1	1.0				

[a] The standard deviation of any of the four replicates tested on two separate occasions was less than 0.34. pEC$_{50}$ = −log 10[EC$_{50}$(M)], where EC$_{50}$ was determined from four parameter fit dose−response curves within an automated fitting program.

Variation of predominantly hydrophobic substituents has some effect (compounds **15** and **16**), but altering the vector of the hydrophobe (compounds **17** and **18**) is detrimental to

Table 3. The Effect of Variation of the Amide Substituent on Binding to Aminergic Receptors[a]

	receptor			
	pEC$_{50}$	pK$_i$		
compd	MrgX1	5-HT2A	5-HT2B	5-HT2C
22	7.6	5.53	5.77	5.81
23	7.3	<5.13	<5.32	<5.22
1	6.9	7.28	7.01	6.52

[a] The standard deviation of the agonist activity at MrgX1 over the six replicates tested on three separate occasions was <0.1. The standard deviation of the binding affinity of the compounds at the 5-HT2 receptors was <0.3 over at least 3 replicates.

potency. Hydrogen bond acceptors close to the meta- position of the distal aromatic ring are beneficial to both potency and intrinsic activity (compounds **19−21**), but the most effective substituents contain both hydrogen bond acceptors and donors in this region (compounds **22** pEC$_{50}$ = 7.6 and **23** pEC$_{50}$ = 7.3).
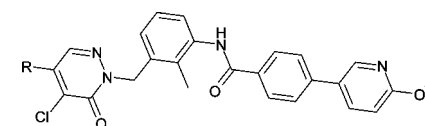
The specificity of the hydrogen bond donor/acceptor interaction for MrgX1 is demonstrated by the reduced affinity of the new ligands for aminergic receptors (Table 3). Whereas the HTS hit (**1**) is equipotent at MrgX1 and 5-HT2, the agonists **22** and **23** show at least 15-fold selectivity for MrgX1 over the 5-HT2 receptors. Docking of the agonist **22** into the MrgX1 model is shown in Figure 1, where the principal putative interactions with the receptor have been highlighted.
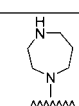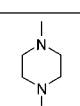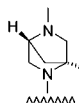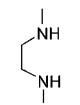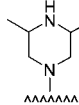
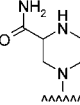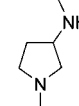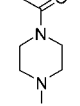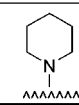**Examination of the Piperazine Module.** The resin based synthesis was adapted to solution phase (Scheme 2) so that a variety of amines could be added to the 4-position of the pyridazinone ring as the final step in the synthesis. ^{1}H and ^{13}C NMR analysis of the final product showed that the modifications to the synthesis had not altered the regioselectivity of the aromatic substitution or alkylation reactions.

It was rapidly apparent from the results of testing the products (Table 4) that the original piperazine ring was the best substituent at the 4-position of the pyridazinone ring.
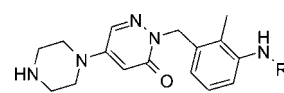
Homopiperazine was tolerated (compound **27**), and methylation, bridging, or opening of the piperazine ring were only slightly detrimental to activity (compounds **28−30**), but bulky substitution around the basic amine markedly reduced activity (compounds **31** and **32**) as did replacement of the piperazine with 3-methylaminopyrrolidine (compound **33**). Removal of the strong positive charge destroyed MrgX1 activity (compounds **34** and **35**). These results suggested that further efforts to improve the piperazine substituent were unlikely to be rewarded and other aspects of the ligand docked into the receptor should be examined as candidates for modification.
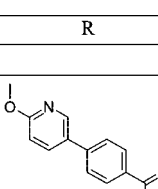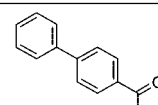
The optimal docking mode for compound **22** into MrgX1 shows the chlorine on the pyridazinone ring pointing away from and making no significant interaction with the receptor. Substitution of hydrogen for this chlorine should not affect hydrophobic binding of the ligand to the receptor and will increase the positive charge on the adjacent nitrogen at physiological pH, strengthening its interaction with the acidic residues of the receptor. The chlorine was removed from compounds **22** and **1** by catalytic hydrogenation (Scheme 2) to provide compounds **36** and **37**, and the structure and regiochemistry of compound **36** was confirmed by ^{1}H and ^{13}C NMR experiments employing HMBC and NOE correlations. In both cases, the removal of the chlorine atom from the pyridazinone ring improved the potency of the compounds for MrgX1 more than 5-fold (Tables 3 and 5) and further reduced their affinity for 5-HT2 receptors. Compound **36** is a full agonist at MrgX1 with a potency in the tens of nanomolar and only weak interaction with 5-HT2B in the micromolar range. This compound was

Table 4. The Effect of Variation of the Piperazine Substituent on MrgX1 Activity[a]

compd	R	pEC$_{50}$	compd	R	pEC$_{50}$
27		7.09	**28**		6.91
29		6.97	**30**		6.53
31		5.24	**32**		5.15
33		5.67	**34**		4.49
35		Inactive			

[a] The standard deviation of the two replicates for each of the above determinations was <0.4.

Table 5. Aminergic Activity of the Dechlorinated MrgX1 Agonists[a]

compd	R	MrgX1	5-HT2A	5-HT2B	5-HT2C
		pEC$_{50}$	pK$_i$		
36		8.2	< 5	6.04	< 5
37		7.7	7.02	7.19	5.55

[a] The standard deviation of the agonist activity of these compounds at MrgX1 in any of the six replicates tested on three separate occasions was <0.13. The standard deviation of the binding affinity of compounds **36** and **37** at the 5-HT2 receptors was <0.3 over 6 and 3 replicates, respectively.

tested against a panel of 50 receptors (CEREP) and found to be inactive at all of them up to 1 μM concentration. When tested against the rat DRR1 receptor compound **36** together with compounds **1**, **22**, and **26** were found to have no detectable agonist activity.

Conclusion

Investigation into the physiological role of MrgX1 in humans has been hampered by the lack of a close orthologue in lower species. Of the 27 mouse and 9 rat Mrg genes, the rat DRR1 (RN2) is the closest equivalent to the human gene but shares

only 60% of its sequence. Evidence for a shared function between human MrgX1 and rat DRR1 comes from their location on similar cells comprising small afferent fibers of the dorsal root ganglion and from their activation by the same small peptide agonist, BAM8−22.[16] Similar difficulties are encountered with all small mammals in which a pain model has been established and which might otherwise be employed to define the role of MrgX1 in the human.

Our approach to this conundrum has been to design a potent and selective small molecule agonist of MrgX1. The SAR derived from this exercise can be used to define the atomic interactions of the agonist with the receptor that will facilitate comparison of the human with the myriad lower mammal receptors and help to define their functional similarity. Further characterization of the human receptor using this agonist together with site directed mutagenesis will be published in due course.

BAM8−22 is a potent agonist of the rat receptor DRR1 but only a weak agonist of the human receptor MrgX1 ($pEC_{50} = 6.1$). By contrast, the selective MrgX1 agonist, which we have developed, has potent activity against the human receptor and could be used to test the effects of an MrgX1 agonist in preparations of human dorsal root ganglia or as an adjunct to morphine therapy in higher mammals that had developed a degree of tolerance to morphine.

Experimental Section

4-Chloro-5-piperazin-1-yl-pyridazin-3-one hydrochloride 3·HCl. 4,5-Dichloro-3-hydroxypyridazine **2**, (11 g, 67 mmol) and piperazine (5.7 g, 66 mmol) were heated in ethanol solution (150 mL) at 90 °C overnight under a reflux condenser. Filtration yielded the solid **3·HCl** (13 g, 92%). ^{1}H NMR (400 MHz, CDCl₃): δ 3.03 (4H, t, *J* = 4.8 Hz), 3.42 (4H, t, *J* = 4.8 Hz), 7.26 (1H, s), 7.64 (1H, s). ^{13}C NMR (100 MHz, DMSO-*d₆*): δ 46.5, 51.3, 115.9, 131.8, 148.4, 163.2; *m/z* 215 [M + H]⁺.

5-(1-Piperazinyl)-3(2*H*)-pyridazinone 3a. Palladium (10%) on carbon (50% H₂O, 0.1 g) was suspended in a solution of 4-chloro-5-piperazin-1-yl-pyridazin-3-one hydrochloride **3**, (0.5 g, 2.3 mmol) in ethanol (25 mL) and treated at 50 °C with hydrazine hydrate (1 mL, 13 mmol). The suspension was stirred under reflux conditions for 1 h when the hot reaction mixture was filtered through a bed of Kieselguhr and the filtrate evaporated to dryness and azeotroped with water. The residue was dissolved in water and adjusted to pH 11 with NaOH and the resulting solution evaporated to dryness and triturated with a mixture of dichloromethane−MeOH (8:2). The organic layer was separated from the solid and evaporated to dryness to provide the title compound as a white solid (360 mg, 87%). ^{1}H NMR (400 MHz, DMSO-*d₆*): δ 2.93 (4H, t, *J* = 4.8 Hz), 3.46 (4H, t, *J* = 4.8 Hz), 5.77 (1H, d, *J* = 2.8 Hz), 6.2−7.2 (1H, brs), 7.92 (1H, d, *J* = 2.8 Hz), 12.10−12.33 (1H, brs).

1-(4-Chloro-3-oxopyridazin-5-yl)-piperazine 4-Carboxy Wang Resin 4. 4-Chloro-5-piperazin-1-yl-pyridazin-3-one hydrochloride **3·HCl** was suspended in water (50 mL), which was adjusted to pH 11 with 40% NaOH and evaporated to dryness. The solid was extracted with dichloromethane−methanol (8:2) and separated from the liquid by filtration. The filtrate was evaporated to dryness and azeotroped with DMF and toluene and dried in a desiccator to provide **3** (2.4 g, 11.2 mmol). This solid was dissolved in dichloromethane (150 mL) and shaken under argon at room temperature with 2-pyridylcarboxy−Wang resin (4 g, 1.7 mmol/g) overnight. The resin was filtered off and washed three times with each of the following solvents: dichloromethane, THF, methanol−water (1:1), THF, and dichloromethane.

A small portion of the dried resin was treated with 20% TFA in dichloromethane to provide **3** as the trifluoroacetate salt; *m/z* 215 [M + H]⁺.

1-(2-(2-Methyl-3-nitrobenzyl)-4-chloro-3-oxopyridazin-5-yl)-piperazine 4-Carboxy Wang Resin 5. 1-(4-Chloro-3-oxopyridazin-5-yl)-piperazine 4-carboxy Wang resin **4** was suspended in THF (150

mL) and shaken with tetramethylguanidine (2.89 mL, 23 mmol) and 2-methyl-3-nitrobenzyl chloride (8.5 g, 45.8 mmol) at room temperature overnight. The resin was filtered off and washed twice with each of the following solvents: dichloromethane, THF, dichloromethane−methanol (2:1, 1:1), methanol, dichloromethane, ether, dichloromethane.

A sample of this resin (20 mg) was cleaved with 20% TFA in dichloromethane for 1.5 h. The reaction mixture was evaporated to dryness and azeotroped with toluene to give **5a** as a yellow oil (5 mg). ^{1}H NMR (400 MHz, CD₃OD): δ 2.48 (3H, s), 3. 41 (4H, t, *J* = 4.8 Hz), 3.73 (4H, t, *J* = 4.8 Hz), 5.46 (2H, s), 7.34 (1H, t, *J* = 8 Hz), 7.46 (1H, d, *J* = 7.6 Hz), 7.69 (1H, d, *J* = 8 Hz), 7.97 (1H, s). ^{13}C NMR (100 MHz, DMSO-*d₆*): δ 14.5, 43.3 (2C), 46.1(2C), 52.7, 116.0, 123.3, 127.2, 130.2, 132.8, 133.0, 137.9, 147.5, 151.5, 157.6; *m/z* 364 [M + H]⁺. HMBC correlations confimed N2 as the site of alkylation.

1-(2-(2-Methyl-3-aminobenzyl)-4-chloro-3-oxopyridazin-5-yl)-piperazine 4-Carboxy Wang Resin 6. 1-(2-(2-Methyl-3-nitrobenzyl)-4-chloro-3-oxopyridazin-5-yl)-piperazine 4-carboxy Wang resin **5** from the previous preparation was suspended in NMP (100 mL) and shaken with SnCl₂·2H₂O (14.4 g, 64 mmol) at room temperature overnight. The resin was filtered off and washed twice with each of the following solvents: NMP, dichloromethane, dioxan, dioxin−water (2:1, 1:1, 1:2), dioxan, and dichloromethane and dried to give 5.7 g of resin. (1.2 mmol/g).

A sample of this resin (29 mg) was cleaved with 20% TFA in dichloromethane and the supernatant fluid was evaporated and azeotroped with toluene. ^{1}H NMR (400 MHz, CD₃OD): δ 2.37 (3H, s), 3. 39 (4H, t, *J* = 5.2 Hz), 3.69 (4H, t, *J* = 5.2 Hz), 5.40 (2H, s), 7.04 (1H, d, *J* = 7.6 Hz), 7.12−7.23 (2H, m), 7.93 (1H, s); *m/z* 334 [M + H]⁺.

1-(2-(2-Methyl-3-(4-phenylbenzoylamido)-benzyl)-4-chloro-3-oxopyridazin-5-yl)-piperazine 4-Carboxy Wang Resin 7. 1-(2-(2-Methyl-3-aminobenzyl)-4-chloro-3-oxopyridazin-5-yl)-piperazine 4-carboxy Wang resin **6** (500 mg, 0.5 mmol) was suspended in DMF−dichloromethane (1:1, 50 mL) and reacted by shaking with 4-phenylbenzoic acid (300 mg, 1.5 mmol), HOAt (204 mg, 1.5 mmol), and DIC (0.234 mL, 1.5 mmol) at room temperature overnight. The resin was separated from the supernatant fluid and was again reacted with the acylating mixture overnight. The resin was filtered off and washed twice with each of the following solvents: dichloromethane−DMF (1:1), dichloromethane, dichloromethane−methanol (1:1), methanol, dichloromethane, to give 529 mg of dried resin bound title compound **7**.

1-(2-(2-Methyl-3-(4-phenylbenzoylamido)-benzyl)-4-chloro-3-oxopyridazin-5-yl)-piperazine 1. 1-(2-(2-Methyl-3-(4-phenylbenzoylamido)-benzyl)-4-chloro-3-oxopyridazin-5-yl)-piperazine 4-carboxy Wang resin (**7**) (0.25 mg) was reacted with 20% TFA in dichloromethane for 1 h. The supernatant fluid was separated and evaporated to dryness and azeotroped with toluene. Purification of this solid by semipreparative reverse phase chromatography gave the title compound (16 mg). ^{1}H NMR (400 MHz, CD₃OD): δ 2.35 (3H, s), 3. 34 (4H, t, *J* = 5.2 Hz), 3.66 (4H, t, *J* = 5.2 Hz), 5.44 (2H, s), 7.14 (1H, d, *J* = 6.8 Hz), 7.21 (1H, t, *J* = 7.6), 7.30 (1H, d, *J* = 8.0 Hz), 7.40 (1H, t, *J* = 7.2), 7.48 (2H, t, *J* = 7.4), 7.69 (2H, d, *J* = 7.2), 7.79 (2H, d, *J* = 8.4), 7. 94 (1H, s), 8.05 (2H, d, *J* = 8.4); *m/z* 514 [M + H]⁺, *m/z* [C₂₉H₂₈ClN₅O₂H]⁺ found 514.2002, error 1.5 ppm.

Biphenyl-4-carboxylic acid [3-(6-*oxo*-4-piperazin-1-yl-6-pyridazin-1-ylmethyl)-2-methyl-phenyl]-amide 37. Biphenyl-4-carboxylic acid [3-(5-chloro-6-oxo-4-piperazin-1-yl-6-pyridazin-1-ylmethyl)-2-methyl-phenyl]-amide, **1** (136 mg, 0.27 mmol) in ethanol (200 mL) was stirred at 70 °C with 10% Pd−C−H₂O (1:1) (50 mg) and hydrazine hydrate (1 mL) for 7 h. The catalyst was removed by filtration and washed with warm ethanol, and the combined filtrates were evaporated to dryness. Trituration of the solid residue with ether gave substantially pure product as a white solid (130 mg), a portion (40 mg) of which was purified by reverse phase HPLC to give the title compound **37** (10 mg). ^{1}H NMR (400 MHz, CD₃OD): δ 2.33 (3H, s), 3. 34 (4H, t, *J* = 5.2 Hz), 3.66 (4H, t, *J* = 5.2 Hz), 5.35 (2H, s), 6.09 (1H, d, *J* = 2.8 Hz), 7.05 (1H, d, *J* = 7.2 Hz), 7.19

(1H, t, *J* = 7.8), 7.29 (1H, d, *J* = 7.2 Hz), 7.39 (1H, t, *J* = 7.6), 7.48 (1H, t, *J* = 7.2), 7.48 (1H, t, *J* = 7.6), 7.70 (2H, d, *J* = 8.8), 7.78 (2H, d, *J* = 8.4), 8.02 (1H, d, *J* = 2.8 Hz), 8.05 (2H, d, *J* = 8.4 Hz); *m/z* 502.5 [M + Na]⁺.

2-(3-Nitro-2-methylbenzyl)-4,5-dichloropyridazin-3-one 24. Tetramethylguanidine (15 mL, 120 mmol) was added slowly to a solution of 2-methyl-3-nitrobenzyl chloride (12.5 g, 67 mmol) and 4,5-dichloropyridazin-3-one (10 g, 61 mmol) in THF (200 mL). The solution went green immediately and was allowed to stir at room temperature overnight.

The solid precipitate was filtered off and washed with THF, and the combined filtrates were evaporated to dryness. The residue was dissolved in ethyl acetate, washed with 0.5 M HCl, an aqueous solution of NaCl and water, dried with magnesium sulfate, and evaporated to dryness. The crude product was recrystalised from *t*-butylmethylether to give 7.93 g of the title compound **24** as a highly crystalline yellow solid. ¹H NMR (400 MHz, CDCl₃): δ 2.54 (3H, s), 5.43 (2H, s), 7.30 (1H, t, *J* = 8 Hz), 7.57 (1H, d, *J* = 7.7 Hz), 7.71 (1H, d, *J* = 8 Hz), 7.80 (1H, s).

2-(3-Amino-2-methylbenzyl)-4,5-dichloropyridazin-3-one 25. Stannous chloride dihydrate (18.6 g, 82.7 mmol) was added to a solution of 2-(3-nitro-2-methylbenzyl)-4,5-dichloropyridazin-3-one, **24** (5.2 g, 16.5 mmol), in ethanol (400 mL) and the mixture was stirred overnight. A further aliquot of stannous chloride was added (5 g, 22 mmol) and the solution was stirred for a further 24 h when the reaction mixture was evaporated to dryness. The residue was shaken with dichloromethane and aqueous sodium bicarbonate, and the organic layer was separated from the resulting emulsion and evaporated to dryness to give the title compound **25** as a yellow solid (4 g). ¹H NMR (400 MHz, CDCl₃): δ 2.19 (3H, s), 3.64 (2H, br s) 5.36 (2H, s), 6.66 (1H, d, *J* = 7.6 Hz), 6.75 (1H, d, *J* = 7.6 Hz), 6.99 (1H, t, *J* = 7.6 Hz), 7.76 (1H, s); *m/z* 285 [M + H]⁺, 306 [M + Na]⁺.

N-[3-(4,5-Dichloro-6-*oxo*-6*H*-pyridazin-1-ylmethyl)-2-methyl-phenyl]-4-(6-methoxy-pyridin-3-yl)-benzamide 26. 2-(3-Amino-2-methylbenzyl)-4,5-dichloropyridazin-3-one, **25** (1 g, 3.5 mmol) was added to a mixture of HOAt (1.36 g, 10 mmol), dicyclohexylcarbodiimide (1.08 mL, 6.9 mmol), and 4-(6-methoxypyridin-3-yl)benzoic acid (2.4 g, 10.4 mmol), which had been stirred in a mixture of dichloromethane−DMF (1:1; 50 mL) for 1 h. After stirring overnight, the reaction mixture was diluted with ether (400 mL) and the title compound **26** (1 g) was filtered off and washed with ether. ¹H NMR (400 MHz, DMSO-*d₆*): δ 2.22 (3H, s), 3.92 (3H, s) 5.37 (2H, s), 6.96 (1H, d, *J* = 8.4 Hz), 7.01 (1H, d, *J* = 7.2 Hz), 7.19 (1H, t, *J* = 8.0 Hz), 7.29 (1H, d, *J* = 7.2 Hz), 7.84 (2H, d, *J* = 8.4 Hz), 8.08 (2H, d, *J* = 8.4 Hz), 8.12 (1H, d, *J* = 8.8 Hz), 8.27 (1H, s), 8.60 (1H, d, *J* = 2.4 Hz) 10.00 (1H, s); *m/z* 495, 497 [M + H]⁺, 517, 519 [M + Na]⁺.

N-[3-(5-Chloro-6-*oxo*-4-piperazin-1-yl-6*H*-pyridazin-1-ylmethyl)-2-methyl-phenyl]-4-(6-methoxy-pyridin-3-yl)-benzamide 22. N-[3-(4,5-Dichloro-6-*oxo*-6 *H*-pyridazin-1-ylmethyl)-2-methyl-phenyl]-4-(6-methoxy-pyridin-3-yl)-benzamide **26** (300 mg, 0.55 mmol) and piperazine (57 mg, 0.66 mmol) were dissolved in DMF (50 mL) and stirred overnight. The reaction mixture was evaporated to dryness and the residue was triturated with ether (200 mL) to give the crude product **22** (400 mg). An aliquot of this material (40 mg) was purified by reverse phase chromatography to provide the title compound **22** (12 mg). ¹H NMR (400 MHz, DMSO-*d₆*): δ 2.19 (3 H, s) 3.02−3.18 (4 H, m) 3.48−3.61 (4 H, m) 3.89 (3 H, s) 4.0−5.5 (2H, br s, exchange) 5.28 (2 H, s) 6.89−6.98 (2 H, m) 7.17 (1 H, t, *J* = 7.6 Hz) 7.31 (1H, d, *J* = 8.8 Hz) 7.80 (2H, d, *J* = 8.33 Hz) 7.97 (1H, s) 8.04 (2H, d, *J* = 8.22 Hz) 8.07 (1H, dd, *J* = 2.52 and 8.8 Hz) 8.28 (1H, br s) 8.54 (1H, d, *J* = 2.3 Hz) 10.09 (1H, s, exchange); *m/z* 567 [M + Na]⁺; *m/z* found 545.20614, C₂₉H₃₀ClN₆O₃ requires 545.20624.

N-[3-(6-*oxo*-4-Piperazin-1-yl-6*H*-pyridazin-1-ylmethyl)-2-methyl-phenyl]-4-(6-methoxy-pyridin-3-yl)-benzamide 36. N-[3-(5-Chloro-6-oxo-4-piperazin-1-yl-6*H*-pyridazin-1-ylmethyl)-2-methyl-phenyl]-4-(6-methoxy-pyridin-3-yl)-benzamide, **22** unpurified from the previous preparation (20 mg, *ca.* 0.36 mmol), was stirred at 70 °C for 3 h as a suspension with hydrazine hydrate (0.2 mL) and 10%

Pd−C/H₂O (1:1, 20 mg). The catalyst was removed by filtration of the warm reaction mixture and, after evaporation of the solvent, the residue was purified by reversed phase chromatography. Trituration of the resulting solid with ether gave the title compound **36** (7 mg). ¹H NMR (500 MHz, DMSO-*d₆*): δ 2.20 (3H, s), 2.43 (1H, br. s.), 2.76 (t, *J* = 4.9 Hz, 4 H), 3.26 (t, *J* = 5.1 Hz, 4 H), 3.92 (s, 3 H), 5.20 (s, 2 H), 5.86 (d, *J* = 2.8 Hz, 1 H), 6.88 (d, *J* = 7.5 Hz, 1 H), 6.96 (d, *J* = 8.6 Hz, 1 H), 7.17 (t, *J* = 7.8 Hz, 1 H), 7.24 (d, *J* = 7.7 Hz, 1 H), 7.84 (d, *J* = 8.4 Hz, 2 H), 8.03 (d, *J* = 2.9 Hz, 1 H), 8.08 (d, *J* = 8.3 Hz, 2 H), 8.12 (dd, *J* = 8.6, 2.6 Hz, 1 H), 8.60 (d, *J* = 2.5 Hz, 1 H), 10.00 (s, 1 H). ¹³C NMR (126 MHz, DMSO-*d₆*): δ 13.5 (s), 44.9 (s), 46.6 (s), 50.6 (s), 53.3 (s), 99.2 (s), 110.6 (s), 125.3 (s), 125.6 (s), 126.1 (s), 126.1 (s), 128.2 (s), 128.3 (s), 129.8 (s), 132.3 (s), 133.0 (s), 136.5 (s), 136.5 (s), 137.6 (s), 139.8 (s), 145.0 (s), 150.0 (s), 160.2 (s), 163.4 (s), 164.8 (s); *m/z* 533 [M + Na]⁺, 511 [M + H]⁺; *m/z* found 511.24508, C₂₉H₃₁N₆O₃ requires 511.24522.

Measurement of MrgX1 Activation by Putative Agonists. Adherent HEK293 cells stably expressing the MrgX1 gene, were seeded into black walled clear-base 384 well plates (Costar UK) at a density of 20000 cells per well in minimum essential medium with Earle's salts and L-glutamine (Gibco 31095-029), supplemented with 10% fetal bovine serum (Gibco 16000-044), 1% nonessential amino acids (Gibco 11140-035) and 50 mg/mL Geneticin (Gibco 10131-027) and cultured overnight. The cells were then incubated with media containing the cytoplasmic calcium indicator, Fluo-4AM (2 μM) and extracellular quenching dye and 2.5 mM probenecid at 37 °C for 60 min. The cells were washed twice with, and finally resuspended in, Tyrode's medium containing 2.5 mM probenecid, The plates were then placed into a FLIPR (Molecular Devices, UK) to monitor cell fluorescence (ex = 488 nM, EM = 540 nM) before and after the addition of the test solutions. Responses were measured as the maximum fluorescent count reached minus the averaged baseline before compound addition. Data was analyzed using a 0.25 IA level for single shot hits or had curves fitted using a four-parameter logistic equation for dose response experiments.

Intrinsic activity was calculated by taking an average of 16 maximal BAM6-22 responses and expressing the maximal response observed by the test compounds as a fraction of this value between 0 and 1.

Supporting Information Available: NMR data for compounds **3a**, **5a**, and **36**. Purity data for all resin unbound compounds. CEREP screening data for compound **36**. MrgX1 computational model with bound ligand compound **22**. This material is available free of charge via the Internet at http://pubs.acs.org.

References

(1) Butera, J. A. Current and Emerging Targets to Treat Neuropathic Pain. *J. Med. Chem.* **2007**, *50*, 2543–2546.

(2) Kennedy, J. D. Neuropathic Pain: Molecular Complexity Underlies Continuing Unmet Medical Need. *J. Med. Chem.* **2007**, *50*, 2547–2556.

(3) Childers, W. E.; Baudy, R. B. N-Methyl-D-Aspartate Antagonists and Neuropathic Pain: The Search for Relief. *J. Med. Chem.* **2007**, *50*, 2557–2562.

(4) Field, M. J.; Li, Z.; Schwarz, J. B. Ca²⁺ Channel α2-δ Ligands for the Treatment of Neuropathic Pain. *J. Med. Chem.* **2007**, *50*, 2569–2575.

(5) Munro, G.; Dalby-Brown, W. Kv7 (KCNQ) Channel Modulators and Neuropathic Pain. *J. Med. Chem.* **2007**, *50*, 2576–2582.

(6) Kyle, D. J.; Ilyin, V. I. Sodium Channel Blockers. *J. Med. Chem.* **2007**, *50*, 2583–2588.

(7) Westaway, S. M. The Potential of Transient Receptor Potential Vanilloid Type 1 Channel Modulators for the Treatment of Pain. *J. Med. Chem.* **2007**, *50*, 2589–2596.

(8) Schkeryantz, J. M.; Kingston, A. E.; Johnson, M. P. Prospects for Metabotropic Glutamate 1 Receptor Antagonists in the Treatment of Neuropathic Pain. *J. Med. Chem.* **2007**, *50*, 2563–2568.

(9) Lai, J.; Luo, M-c.; Chen, Q.; Porreca, F. Pronociceptive actions of dynorphin via bradykinin receptors. *Neurosci. Lett.* **2008**, *437*, 175–179.

(10) Coa, H.; Zhang, Y-Q. Spinal glial activation contributes to pathological pain states. *Neurosci. Biobehav. Rev.* **2008**, *32*, 972–983.

(11) Burns, J. W.; Quartana, P. J.; Bruehl, S. Anger inhibition and pain: conceptualizations, evidence and new directions. *J. Behav. Med.* **2008**, *31*, 259–279.

(12) Guindon, J.; Walczak, J-S.; Beaulieu, P. Recent Advances in the Pharmacological Management of Pain. *Drugs* **2007**, *67*, 2121–2133.

(13) Newsome, S.; Frawley, B. K.; Argoff, C. E. Intrathecal analgesia for refractory cancer pain. *Curr. Pain Headache Rep.* **2008**, *12*, 249–256.

(14) Dong, X.; Han, S.; Zylka, M. J.; Simon, M. I.; Anderson, D. J. A diverse family of GPCRs expressed in specific subsets of nociceptive sensory neurons. *Cell* **2001**, *106*, 619–632.

(15) Lembo, P. M. C.; Grazzini, E; Groblewski, T.; O'Donnell, D.; Roy, M-O.; Zhang, J.; Hoffert, C.; Cao, J.; Schmidt, R.; Pelletier, M.; Labarre, M.; Gosselin, M.; Fortin, Y.; Banville, D.; Shen, S. H.; Strom, P.; Payza, K.l; Dray, A.; Walker, P.; Ahmad, S. Proenkephalin A gene products activate a new family of sensory neuron-specific GPCRs. *Nat. Neurosci.* 2002 *5*, 201–209.

(16) Grazzini, E.; Puma, C.; Roy, M-O.; Yu, X. H.; O'Donnell, D.; Schmidt, R.; Dautrey, S.; Ducharme, J.; Perkins, M.; Panetta, R.; Laird, J. M. A.; Ahmad, S.; Lembo, P. M. C. Sensory neuron-specific receptor activation elicits central and peripheral nociceptive effects in rats. *Proc. Natl. Acad. Sci. U.S.A.* **2004**, *101*, 7175–7180.

(17) Yang, S.; Liu, Y.; Lin, A. A.; Cavalli-Sforza, L. L.; Zhao, Z.; Su, B. Adaptive evolution of MRGX2, a human sensory neuron specific gene involved in nociception. *Gene* **2005**, *352*, 30–35.

(18) Zylka, M. J.; Dong, X.; Southwell, A. L.; Anderson, D. J. Atypical expansion in mice of the sensory neuron-specific MrgG protein-coupled receptor family. *Proc. Natl. Acad. Sci. U.S.A.* **2003**, *100*, 10043–10048.

(19) Burstein, E. S.; Ott, T. R.; Feddock, M.; Ma, J-N.; Fuhs, S.; Wong, S.; Schiffer, H. H.; Brann, M. R.; Nash, N. R. Characterization of the Mas-related gene family: structural and functional conservation of human and rhesus MrgX receptors. *Br. J. Pharmacol.* **2006**, *147*, 73–82.

(20) Zhang, L.; Taylor, N.; Xie, Y.; Ford, R.; Johnson, J.; Paulsen, J. E.; Bates, B. Cloning and expression of MRG receptors in macaque, mouse and human. *Mol. Brain Res.* **2005**, *133*, 187–197.

(21) Kunapuli, P.; Lee, S.; Zheng, W.; Alberts, M.; Kornienko, O.; Mull, R.; Kreamer, A.; Hwang, J. I.; Simon, M. I.; Strulovici, B. Identification of small molecule antagonists of the human mas-related gene-X1 receptor. *Anal. Biochem.* **2006**, *351*, 50–61.

(22) Tomaszewski, M. ; Discovery of pain targets—GPCR target class approach, XVIII International Symposium on Medicinal Chemistry, Copenhagen, Denmark, August, 2004.

(23) Cai, Q.; Jiang, J.; Chen, T.; Hong, Y. Sensory neuron-specific receptor agonist BAM8−22 inhibits the development and expression of tolerance to morphine in rats. *Behav. Brain Res.* **2007**, *178*, 154–159.

(24) Teitelbaum, H.; Catravas, G. N.; McFarland, W. L. Reversal of morphine tolerance after medial thalamic lesions in the rat. *Science* **1974**, *185*, 449–451.

(25) Guo, R-x.; Cui, Y.; Mo, L-q.; Liu, W.; Feng, J-q. Changes of the spinal δ opioid receptors and NMDA receptors during the development of morphine tolerance. *Jiepouxue Yanjiu* **2007**, *29*, 88–92.

(26) Mendez, I. A.; Trujillo, K. A. NMDA receptor antagonists inhibit opiate antinociceptive tolerance and locomotor sensitization in rats. *Psychopharmacology (Berlin, Ger.)* **2008**, *196*, 497–509.

(27) Dalton, G. D.; Smith, F. L.; Smith, P. A.; Dewey, W. L. Alterations in brain protein kinase A activity and reversal of morphine tolerance by two fragments of native protein kinase A inhibitor peptide (PKI). *Neuropharmacology* **2005**, *48*, 648–657.

(28) Parkitna, J. R.; Obara, I.; Wawrzczak-Bargiela, A.; Makuch, W.; Przewlocka, B.; Przewlocki, R. Effects of glycogen synthase kinase 3 and cyclin-dependent kinase 5 inhibitors on morphine-induced analgesia and tolerance in rats. *J. Pharmacol. Exp. Ther.* **2006**, *319*, 832–839.

(29) Smith, F. L.; Javed, R.; Elzey, M. J.; Welch, S. P.; Selley, D.; Sim-Selley, L.; Dewey, W. L. Prolonged reversal of morphine tolerance with no reversal of dependence by protein kinase C inhibitors. *Brain Res.* **2002**, *958*, 28–35.

(30) Adam, F.; Dufour, E.; Le Bars, D. The glycine site-specific NMDA antagonist (+)-HA966 enhances the effect of morphine and reverses morphine tolerance via a spinal mechanism. *Neuropharmacology* **2008**, *54*, 588–596.

(31) Chen, T.; Hu, Z.; Quirion, R.; Hong, Y. Modulation of NMDA receptors by intrathecal administration of the sensory neuron-specific receptor agonist BAM8−22. *Neuropharmacology* **2008**, *54*, 796–803.

(32) Olsson, R.; Knapp, A. E.; Eskildsen, J. Preparation of benzimidazole derivatives, especially N2-derivatized argininamides containing a substituted benzimidazole unit as modulators of MrgX receptors for the treatment of pain and methods of screening them. Patent WO2008052072, 2008.

(33) Sullivan, E.; Tucker, E. M.; Dale, I. L. Measurement of [Ca^{2+}] using the fluorometric imaging plate reader (FLIPR). *Methods Mol. Biol.* **1999**, *114*, 125–133.

(34) Sali, A.; Blundell, T. L. Comparative protein modeling by satisfaction of spatial restraints. *J. Mol. Biol.* **1993**, *234*, 779–815.

(35) McMartin, C.; Bohacek, R. S. QXP: powerful, rapid computer algorithms for structure-based drug design. *J. Comput.-Aided Mol. Des.* **1997**, *11*, 333–344.

(36) Rauhut, G.; Clark, T. Multicenter point charge model for high-quality molecular electrostatic potentials from AM1 calculations. *J. Comput. Chem.* **1993**, *14*, 503–509.

(37) Schwartz, T. W.; Frimurer, T. M.; Holst, B.; Rosenkilde, M. M.; Elling, C. E. Molecular mechanism of 7TM receptor activation—a global toggle switch model. *Annu. Rev. Pharmacol. Toxicol.* **2006**, *46*, 481–519.